PROCEEDINGS B

royalsocietypublishing.org/journal/rspb

Research

Cite this article: Haynes KJ, Walter JA, Liebhold AM. 2019 Population spatial synchrony enhanced by periodicity and low detuning with environmental forcing. *Proc. R. Soc. B* **286**: 20182828.
http://dx.doi.org/10.1098/rspb.2018.2828

Received: 12 December 2018
Accepted: 7 May 2019

Subject Category:
Ecology

Subject Areas:
ecology

Keywords:
population cycles, frequency detuning, Moran effect, phase locking, spatial synchrony, timescale

Author for correspondence:
Kyle J. Haynes
e-mail: haynes@virginia.edu

Electronic supplementary material is available online at https://dx.doi.org/10.6084/m9.figshare.c.4506743.

THE ROYAL SOCIETY PUBLISHING

Population spatial synchrony enhanced by periodicity and low detuning with environmental forcing

Kyle J. Haynes[1,2], Jonathan A. Walter[2] and Andrew M. Liebhold[3,4]

[1]The Blandy Experimental Farm, University of Virginia, Boyce, VA, USA
[2]Department of Environmental Sciences, University of Virginia, Charlottesville, VA, USA
[3]US Forest Service Northern Research Station, Morgantown, WV 26505, USA
[4]Czech University of Life Sciences Prague, Faculty of Forestry and Wood Sciences, Praha 6 - Suchdol, Czechia 16521, Czech Republic

KJH, 0000-0002-3283-6633; JAW, 0000-0003-2983-751X; AML, 0000-0001-7427-6534

Explaining why fluctuations in abundances of spatially disjunct populations often are correlated through time is a major goal of population ecologists. We address two hypotheses receiving little to no testing in wild populations: (i) that population cycling facilitates synchronization given weak coupling among populations, and (ii) that the ability of periodic external forces to synchronize oscillating populations is a function of the mismatch in timescales (detuning) between the force and the population. Here, we apply new analytical methods to field survey data on gypsy moth outbreaks. We report that at timescales associated with gypsy moth outbreaks, spatial synchrony increased with population periodicity via phase locking. The extent to which synchrony in temperature and precipitation influenced population synchrony was associated with the degree of mismatch in dominant timescales of oscillation. Our study provides new empirical methods and rare empirical evidence that population cycling and low detuning can promote population spatial synchrony.

1. Introduction

Correlation through time in the fluctuating abundances of a given species among populations separated by space, known as 'population spatial synchrony', is pervasive [1] and has important implications for species conservation [2] and the impacts and management of pest species [3]. The most striking examples of this phenomenon tend to involve species that exhibit locally cyclical fluctuations in abundance (e.g. Canada lynx [4] and Finnish tetraonids [5]), suggesting that population cycles may facilitate population spatial synchrony [6]. Bjørnstad [7, p. 872] compared patterns of spatial synchrony in several different systems and concluded 'cyclic populations yearn to align themselves'.

Theory indicates the degree to which spatially disjunct populations are prone to synchronization can depend on whether local populations exhibit stable, cyclic or chaotic dynamics [7,8]. Cyclic dynamics, in particular, are predicted to promote the synchronization of weakly coupled populations, owing in part to the occurrence of phase locking. Phase locking (otherwise known as phase synchronization) is an important stage in the process of synchronization in which the phases of populations become entrained [9,10]. The prediction that cyclic dynamics are easily synchronized has held true when the coupling between populations was modelled as low rates of dispersal [6–8,11] as well as locally synchronous environmental variation [8,12]. Laboratory experiments using *in vitro* populations of protists confirmed that population cycles, which were induced by predator–prey interactions, allowed dispersal to bring populations into synchrony [6]. In chaotic populations, dispersal [9] or exogenous environmental forces (e.g. weather) [13] can lead to partial synchronization in which the populations become phase locked, but their abundances remain

largely uncorrelated. Although in ecology considerable attention has been given to the role of local dispersal as the source of weak coupling underlying phase locking, phase locking is a more general phenomenon that may also be driven by shared impacts from exogenous forces [10,12].

Theoretical predictions that address how the synchrony of oscillators is affected by the nature of exogenous forces—their strengths, periodicities and frequencies—have been central to several advances in fields such as physiology and electrical and radio engineering [10,14], but predictions that appear highly relevant to the study of population synchronization have received less attention in ecological studies. For example, in systems of periodic oscillators (e.g. local cyclical populations) and periodic external forcing, the degree to which the external force synchronizes the oscillators should depend, in large part, on the difference between the frequency of the external force and the frequency of population oscillations. For weak to moderate forces, the larger the difference between the frequency of the external force and the frequency of the oscillators (a quantity termed 'detuning'), the stronger the force must be to synchronize the oscillators [10,14]. In the context of cyclical populations, therefore, a weather variable that displays periodicity in its fluctuations at a frequency that closely matches that of the populations (low detuning) might be a stronger agent of population synchronization than a weather variable that is periodic but at a timescale that does not closely match the timescale of population fluctuations.

Despite theoretical predictions and experimental evidence, the extent to which cyclic dynamics in field populations promote population spatial synchrony is largely unknown. As reviewed by Bjørnstad [7], the main empirical evidence used to address this question stems from 'historical experiments', such as past vaccination or predator-extermination programmes, in which human intervention altered the periodicity of population dynamics and changes in spatial synchrony followed [15,16]. Perhaps the most convincing evidence from field populations that periodic population dynamics promote population spatial synchrony is Henden *et al.*'s [17] study of fox bounty data in Norway. They found that cyclical populations displayed greater spatial synchrony than non-cyclical populations. However, no methodology has been developed to isolate cycle-induced population spatial synchrony from generic population time-series data.

Here, we harness extensive data on gypsy moth outbreaks across deciduous forests in eastern North America over a 26-year period to test whether the spatial synchrony of outbreaks increases with their periodicity within local neighbourhoods. Gypsy moth populations can be characterized as cyclic, nonlinear oscillators in that they exhibit periodic abundance fluctuations which are thought to arise primarily from host–pathogen dynamics [18,19]; there is no evidence that periodicity in meteorological factors are significant drivers of periodicity of gypsy moth populations. However, previous work showed that synchrony in precipitation is a likely driver of synchrony in gypsy moth outbreaks [20,21]. Therefore, in this study we examined the combined effects of synchrony in weather and population cycling on the synchrony of gypsy moth outbreaks.

Synchrony at a given timescale (period length) may not be indicative of synchrony at other timescales [22]. Consequently, simple correlation-based measures of synchrony may be inadequate [22]. Given that gypsy moth populations in the northeastern United States have been shown to exhibit harmonic oscillations at multiple period lengths [23], we examined the drivers of gypsy moth population spatial synchrony at the dominant timescales of gypsy moth cycles. We tested the predictions that the phase synchrony and synchrony in the abundance of a focal population with neighbouring populations would increase with the periodicity of the neighbouring populations, while accounting for known synchronizing effects of weather on gypsy moth outbreaks. Using novel statistical methods for quantifying local heterogeneity in synchrony at various timescales, we demonstrate in field populations the existence of relationships between population periodicity, phase locking, and synchrony and investigate the potential for detuning to determine the synchronizing effects of environmental forces.

2. Material and methods

(a) Study system

The gypsy moth is a highly polyphagous foliage-feeding forest insect native to Eurasia. In eastern deciduous forests of North America, where it is non-native and invasive, it periodically reaches epidemic levels resulting in extensive forest defoliation [24] that is partially synchronous over several hundred kilometres [25,26]. While exact causes of population cycles are not known, a probable mechanism is density-dependent mortality from the gypsy moth nucleopolyhedrosis virus (*Ld*NPV) [19,27]. Since *ca* 1989, the fungal pathogen *Entomphaga maimaiga* has become the dominant cause of gypsy moth mortality [28], but given that most evidence suggests this mortality is density independent [29,30], *E. maimaiga* may not be a driver of gypsy moth population cycles.

(b) Defoliation and weather data

We used digitized data from annual aerial surveys of gypsy moth defoliation from 1990 to 2015 (electronic supplementary material, figure S1) to examine relationships between the periodicity and synchrony of outbreaks. (See a flowchart describing the workflow we followed in our analyses in electronic supplementary material, figure S2.) Given the low dispersal ability of gypsy moths—adult females are flightless and ballooning 1st instar larvae typically disperse only tens of metres [31]—we examined this aerial survey data at a finer spatial scale (8 × 8 km grid cells) than previous studies of synchrony in gypsy moth dynamics [20,21,25,26]. Based on previous research showing a positive correlation between the area of forest defoliated and gypsy moth egg masses [32,33], we used the proportion of defoliated area (km^2) in a given year as a proxy of gypsy moth abundance within each cell.

We only used defoliation data from areas that had been invaded by the gypsy moth prior to 1990 as defined by the United States (US) Department of Agriculture quarantine declarations (US Code of Federal Regulations, Title 7, Chapter III, §01.45). Because our motivation was to test whether spatial synchrony of outbreaks increases with their periodicity within local neighbourhoods (which we defined as a focal grid cell and its 1–8 adjacent neighbour grid cells), and it is not possible to quantify periodicity from time series in which gypsy moth defoliation levels are almost entirely zero, we limited all of our analyses to 1327 of 10 569 focal grid cells (electronic supplementary material, figure S1) in which defoliation was detected in 4 or more years both in the focal grid cell and at least 1 of the 8 adjacent neighbour grid cells. The excluded grid cells probably had low densities of the gypsy moth's preferred host tree species;

Liebhold *et al*. [34] found a positive correlation between the annual frequency of defoliation and the density of preferred hosts.

Weather data for each of the 1327 grid cells were gathered from the PRISM Climate Group, Oregon State University (http://prism.oregonstate.edu). Monthly weather variables were obtained at a spatial resolution of 4×4 km and averaged across each 8×8 km grid cell. For each month (January–December) from 1990 to 2015, we obtained total precipitation and the means of daily minimum and maximum temperatures for each grid cell. Because the weather data were comprised 36 potentially collinear weather variables (three weather variables across 12 different months), we used principal components analysis (PCA) to reduce its dimensionality, selecting the first two principal components (PC1 and PC2) for analysis. The PCA was conducted using the 'stats' package for R [35].

(c) Spectral analysis of defoliation time series

Wavelet analysis was carried out to characterize the periodicity and timescales of fluctuations in both defoliation and weather (PC1 and PC2) in each grid cell. Wavelet analyses of gypsy moth defoliation data have been published previously, showing complex cyclical behaviour with harmonic oscillations with timescales (period lengths) of 4–5 and 8–10 years [23], but the prior analyses examined defoliation data that were both less recent and from a smaller geographical area (i.e. areas invaded before 1974) than we analysed in the current study (here, we limited our analysis to areas invaded before 1990). Wavelet power at a given timescale quantifies the matching between a time series and a wavelet function exhibiting oscillations at the same timescale. The wavelet function we used was the continuous Morlet wavelet [36]. Following Liu *et al*. [37], we corrected the power spectra (by dividing power values by the wavelet scale) to eliminate a bias in traditional wavelet analysis that imbues greater wavelet power to signals with longer timescales. Prior to conducting the wavelet analyses, we normalized the distributions of the defoliation time series [38] using the power transformation $f(x) = x^t$, with $t = 0.2$. In addition, to account for differences in the amount or variability of defoliation among grid cells, each grid cell's defoliation time series was detrended and standardized to a standard deviation of 1 and mean of 0. To determine the dominant timescales of gypsy moth cycles, we tested the significance of the wavelet power values across the range of timescales considered (2–13 yr) for each grid cell's time series. The wavelet analyses were carried out using Cazelles *et al*.'s [39] package for MATLAB, with significance testing carried out using hidden Markov model simulations [40].

(d) Timescale-specific spatial synchrony

We examined local heterogeneity in timescale-specific spatial synchrony of gypsy moth defoliation by applying two metrics that quantify synchrony in distinct, complementary ways. First, we developed a cross-wavelet-based extension of non-centred local indicators of spatial association (ncLISA; [41]). This approach is similar to the timescale-specific decomposition of synchrony in spatial moving windows employed by Defriez & Reuman [22]. Like ncLISA, our approach examines geographies of synchrony [42] by quantifying, for each focal cell, the mean synchrony of a variable (e.g. abundance) between the focal cell and all other cells within its local neighbourhood, revealing areas of relatively high and low synchrony. We specified that a local neighbourhood consisted of a focal cell and its (1–8) adjacent cells. Our cross-wavelet version (cross-wavelet ncLISA) replaces a conventional correlational measure of synchrony with the power-normalized real part of the cross-wavelet transform (ReXWT; see for mathematical detail [42]). This metric takes into account both whether the amplitudes of fluctuations are correlated through time and whether the fluctuations are in phase with one another, yielding a timescale-specific measure of synchrony with similar properties to correlation: values of ReXWT span −1 to 1, with perfect negative (antiphase) relationships taking the value -1 and perfect positive (in-phase) relationships taking 1. We hereafter refer to this metric as 'cross-wavelet synchrony' to distinguish between synchrony metrics.

Second, we quantified phase synchrony in the same local neighbourhoods using a second ncLISA analogue. Phase synchrony takes into account only the tendency of oscillations to be in-phase, ignoring oscillation amplitudes. For each local neighbourhood (focal cell and its adjacent neighbour cells), we quantified the mean pairwise phase synchrony between the focal grid cell and each adjacent neighbour over timescale bands of interest. We used wavelet analysis to determine the time-localized and timescale-specific phase of fluctuations in gypsy moth defoliation time series across the entire 26-year length of the time series. Pairwise phase synchrony was given by the expression

$$\frac{1}{N}\sum_{j=1}^{N}\left[\frac{1}{T}\sum_{t=1}^{T}\left[\frac{1}{S}\sum_{\sigma\in s}\bar{R}\left(\phi_{i,t,\sigma},\phi_{j,t,\sigma}\right)\right]\right], \tag{2.1}$$

where $\bar{R}\left(\phi_{i,t,\sigma},\phi_{j,t,\sigma}\right)$ is the mean resultant vector length [43] from vectors of length 1 and phase angles ϕ at focal cell i and neighbouring location j at time t and timescale σ from s, the set of timescales of interest. S is the number of wavelet scales in s, T is the length of the time series (26 years) and N is the number of cells adjacent to the focal cell. Equation (2.1) is a reliable index of phase synchrony at timescale σ because if the vectors from all or most cells within a neighbourhood tend to have phase angles similar to the vector from the focal cell for each year t, the resulting index value will be relatively large, but the value will be small if the phases tend to be uncorrelated through time [44].

We measured cross-wavelet synchrony and phase synchrony of gypsy moth defoliation in local neighbourhoods across the study area at two timescale ranges, 2–4 years and 7–11 years, because wavelet analysis revealed a high prevalence of statistically significant periodicity in defoliation at these period lengths (see Results). As above, we used the continuous complex Morlet wavelet transform [36]. Analyses were carried out in R version 3.5.1 [35] using the 'wsyn' [45] and 'circular' [46] packages and code modified from the 'ncf' library [47].

(e) Factors affecting timescale-specific spatial synchrony of outbreaks

We tested whether local cross-wavelet synchrony in defoliation increased with the periodicity (mean wavelet power) of defoliation in the 1–8 adjacent neighbour cells with weighted generalized-least-squares (WGLS) regressions using the 'nlme' package [48] for R. We used a separate WGLS model for each timescale range (2–4 years and 7–11 years) to evaluate the drivers of synchrony of defoliation at each timescale range. We also assessed if cross-wavelet synchrony in defoliation was influenced by synchronous environmental fluctuations by including local cross-wavelet synchrony (at the corresponding timescale range) in the scores of the two dominant principal components of weather as predictor variables in the two WGLS models. For each timescale range (2–4 years and 7–11 years), we also tested if phase synchrony in defoliation increased with the periodicity of defoliation in the adjacent neighbour cells, or phase synchrony of the two dominant components of weather, using a WGLS model. To account for spatial autocorrelation among cells, we directly modelled the spatial patterns in the residuals of the WGLS regression models. We evaluated WGLS models using different functions for describing the pattern of spatial decay in the autocorrelation of the residuals (Gaussian, exponential or no

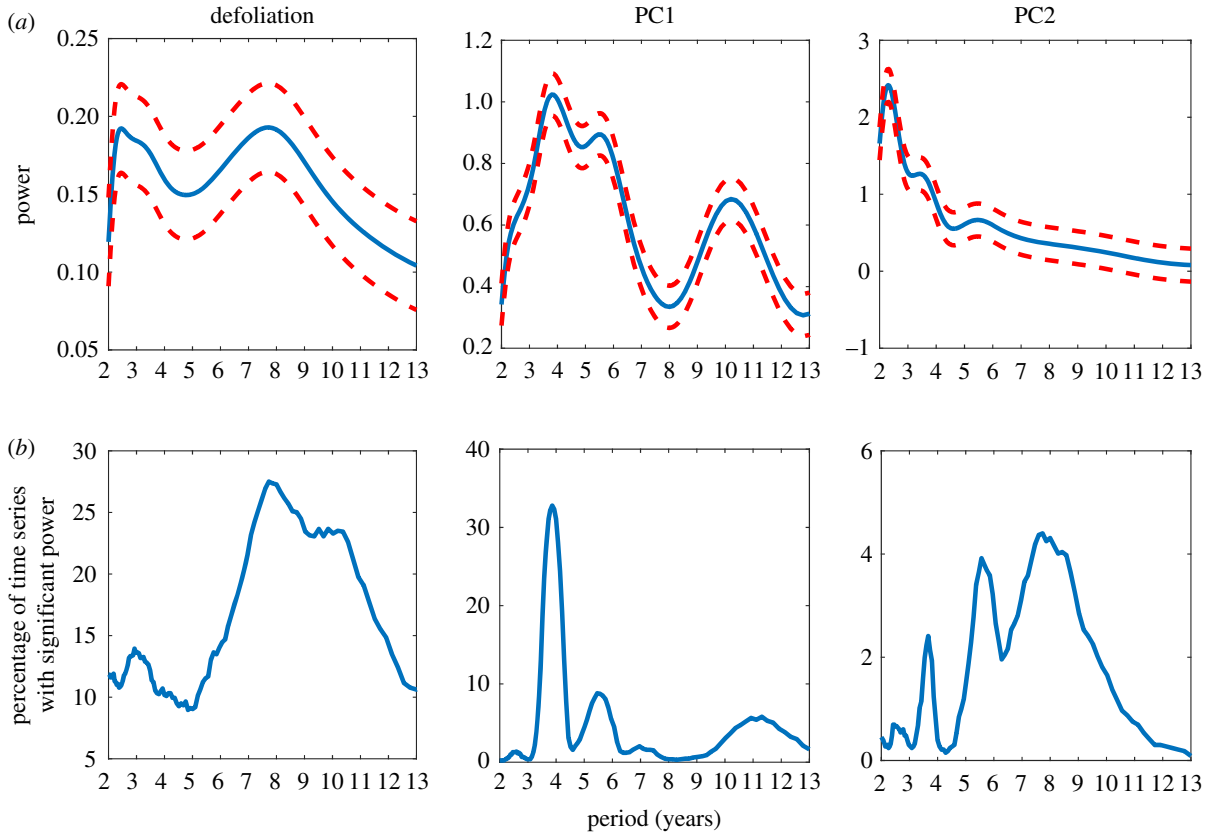

Figure 1. Summary of wavelet analyses on 1327 time series of gypsy moth defoliation and the scores of the first (PC1) and second (PC2) principal components of monthly temperature and precipitation variables, with each time series corresponding to an 8 × 8 km grid cell. (*a*) Mean wavelet power (solid line) and 95% confidence interval (dashed line) are shown. (*b*) The percentage of time series in which the wavelet power was statistically significant at $\alpha = 0.05$ across timescales (period lengths) of 2–13 years. (Online version in colour.)

spatial structure) and selected, for each model (response variable), the function that provided the lowest Akaike's information criterion corrected for small sample size (AICc). The weight for each focal grid cell was the number of grid cells present within its neighbourhood. To normalize the model residuals, mean 2–4 year and 7–11 year cross-wavelet synchronies were Box-Cox transformed (after adding constants of 1.0 and 0.6, respectively, to make all values positive) using exponents (λ) of 1.6 and 4.8 for the respective timescales. Mean 2–4 year and 7–11 year phase synchronies were Box-Cox transformed using λ-values of 1.7 (2–4 year timescale) and 10.7 (7–11 year timescale). Multicollinearity in each model was checked by inspecting variance inflation factors (VIFs). Finally, we assessed whether the WGLS models above, each with three predictor variables (timescale-specific periodicity of defoliation and timescale-specific (cross-wavelet or phase) synchrony in the scores of the two dominant components of weather) provided a better fit to the data than null models (comprised an intercept term and the same error autocorrelation structures as the full models, but no predictor variables) using likelihood ratio tests.

3. Results

(a) Periodicity of gypsy moth outbreaks and weather

The mean wavelet power spectrum of the 1327 defoliation time series was bimodal, with the strongest cycling (periodicity) at period lengths of roughly 2.4 years and 7.8 years (figure 1). Similarly, peaks in the percentage of time series with significant periodicity occurred at period lengths of approximately 3.0 years and 7.8 years. The short timescale peak was confined to a rather narrow timescale bandwidth, but the long timescale peak was broader and featured a distinct 'shoulder-shaped' relationship between the period length and the percentage of time series with significant periodicity at period lengths greater than 9 years. The percentage of time series with significant periodicity was consistently approximately 23% for period lengths of approximately 9.0–10.4 years, but the prevalence of significant periodicity declined rapidly with period length increasing beyond 10.4 years.

In the PCA of weather data, we found the first component (PC1) largely represented temperature, whereas the second component (PC2) primarily explained precipitation (see appendix S1 in the electronic supplementary material). Respectively, PC1 and PC2 explained 41.2% and 7.5% of the total variation in the weather variables.

The mean wavelet power spectrum of PC1 scores exhibited a dominant peak at a period length of approximately 3.8 years, a slightly weaker peak at period lengths of approximately 5.5 years, and a considerably weaker peak at approximately 10 years (figure 1). The time series of PC1 scores exhibited statistically significant periodicity most frequently at a period length of approximately 3.8 years, but there were also minor peaks in the incidence of significant periodicity at approximately 5.5 and 11.2 years (figure 1). For the time series of PC2 scores, mean wavelet power exhibited a dominant peak at approximately 2.2 years and two substantially weaker peaks at approximately 3.5 and approximately 5.5 years (figure 1). However, significant power in the scores of PC2 was found most frequently at longer timescales ranging roughly from 5–6 and 7–9 years (figure 1).

(b) Factors affecting timescale-specific spatial synchrony of outbreaks

Cross-wavelet synchrony was weaker at 2–4 year timescales (0.48, 0.29–0.65; median, 1st quartile–3rd quartile) than 7–11 year timescales (0.88, 0.72–0.94). Phase synchrony was also weaker at 2–4 year timescales (0.82, 0.76–0.88) than 7–11 year timescales (0.97, 0.91–0.99).

Based on AICc values, the exponential spatial decay function was selected as the best function for modelling the spatial autocorrelation in the residuals of the WGLS models for all response variables (cross-wavelet synchrony and phase synchrony at the 2–4 year and 7–11 year timescales), with the exception of 7–11 year cross-wavelet synchrony, for which the Gaussian spatial decay function was selected. Likelihood ratio tests showed that for all four response variables, the fit of the full WGLS model was significantly better ($p < 0.001$) than the fit of the null WGLS model; each null model comprised an intercept term and the same error autocorrelation structures described above, but no predictor variables. There was little evidence of multicollinearity in the full WGLS models, as the highest VIF across all models was 1.04.

The 2–4 year periodicity of defoliation (mean 2–4 year wavelet power) in grid cells surrounding a focal cell was not a significant predictor of the mean cross-wavelet synchrony of defoliation (at 2–4 year timescales) between the focal grid cell and its neighbouring cells (table 1). The only variable that was a significant predictor of the (mean) cross-wavelet synchrony of defoliation at the 2–4 year timescales was 2–4 year cross-wavelet synchrony in the scores of PC1 (table 1). The relationship between these two variables was negative. For the phase synchrony of defoliation at the 2–4 year timescales, none of the predictor variables were statistically significant (table 2).

Contrasting with the 2–4 year timescales, the 7–11 year cross-wavelet synchrony of defoliation increased significantly with the 7–11 year periodicity of defoliation (table 1) in neighbouring grid cells. The 7–11 year cross-wavelet synchrony of defoliation also increased significantly with the 7–11 year cross-wavelet synchrony in the scores of PC2. Similar to the results for cross-wavelet synchrony at the 7–11 year timescales, the 7–11 year phase synchrony of defoliation increased significantly with the 7–11 year periodicity of defoliation (table 2). However, there was no significant relationship between the 7 and 11 year phase synchrony of PC2 and the 7–11 year phase synchrony of defoliation.

The geographies of periodicity, cross-wavelet synchrony and phase synchrony (figures 2 and 3) reflect the statistical evidence (table 1) of a stronger linkage between periodicity and synchrony at the 7–11 year than at the 2–4 year timescale. Neighbourhoods with strong 2–4 year periodicity (mean wavelet power) in defoliation were strongly concentrated in a portion of central Michigan (figure 2*a*), but diffuse elsewhere. Two-to-four year periodicity was somewhat spatially cohesive with 2–4 year cross-wavelet synchrony within Michigan, but 2–4 year periodicity did not correspond closely with 2–4 year cross-wavelet synchrony or 2–4 year phase synchrony across the rest of the study area (figure 2*b*,*c*). By contrast, neighbourhoods of strong 7–11 year periodicity in defoliation were most strongly concentrated in various areas of central Pennsylvania, West Virginia and New Jersey (figure 3*a*). These areas also tended to have high cross-wavelet synchrony in defoliation at the 7–11 year timescale (figure 3*b*). Seven-to-eleven year periodicity was also fairly spatially cohesive with 7–11 year cross-wavelet synchrony within Michigan (figure 3*a*–*c*), with both variables tending to increase from north to south. Similarly, 7–11 year periodicity was largely spatially cohesive with both 7–11 year cross-wavelet synchrony in the northeastern states of Maine, Massachusetts and Connecticut (figure 3*a*–*c*). Finally, areas with strong 7–11 year periodicity in defoliation (figure 3*a*) also tended to have strong 7–11 year phase synchrony in defoliation (figure 3*c*).

4. Discussion

Consistent with the theoretical prediction that population cycles can bring the fluctuations of local populations weakly linked by dispersal or shared environmental variation into synchrony [6,8,11,12,49], we found a positive relationship (at 7–11 year timescales) across space between the synchrony of gypsy moth defoliation in a focal location (grid cell) with neighbouring gypsy moth populations and the periodicity of defoliation in the neighbouring populations (table 1). Consistent with previous studies [20,21,42], the local synchrony of gypsy moth populations also increased with the synchrony of precipitation, though here we found this association was timescale-specific (i.e. occurring at the 7–11 year timescales but not the 2–4 year timescales; table 1). The association between precipitation synchrony and gypsy moth population synchrony does not necessarily indicate that precipitation is a dominant factor driving gypsy moth dynamics. To the contrary, nonlinearities in density dependence, or the combined effects of dispersal and environmental synchrony, can cause population synchrony to either exceed or fall below environmental synchrony [7,8,12,49,50]. Thus, it is possible that precipitation has a relatively minor effect on gypsy moth dynamics yet a strong synchronizing effect. Nevertheless, there are reports in the literature of precipitation impacting important processes in gypsy moth dynamics. Specifically, precipitation is known to influence transmission and growth of gypsy moth pathogens [51,52].

We also found a positive association across space between the phase synchrony and periodicity of gypsy moth defoliation at the 7–11 year timescales, providing empirical support that gypsy moth population cycles facilitate synchronization via phase locking. Prior studies have reported instances of phase locking, such as when the phases of Canadian lynx population cycles in different provinces synchronize after temporarily slipping out of phase [4,9]; however, this type of observation represents relatively weak evidence of a link between the tendency of populations to cycle (periodicity) and phase locking. With the exception of rare 'historical experiments' [7,15,16], this is, to our knowledge, the first study to yield quantitative evidence that population cycling promotes phase locking in nature. Unlike historical experiments, which rely on a fortuitous disruption in the past to cyclical population dynamics (e.g. through a vaccination programme that altered patterns of epidemics), the approach developed here only requires spatially replicated population time-series data.

Table 1. Results of generalized-least-squares regressions testing whether the timescale-specific local cross-wavelet synchrony of gypsy moth defoliation between a focal location and neighbouring locations increases with the periodicity of defoliation in the neighbouring locations, while accounting for the effects of the local synchrony of weather (scores of two principal components) in neighbouring locations ($n = 1327$). (Significant p-values are highlighted with an asterisk (*).)

dependent variables	independent variables	coef.	s.e.	t	p-value
2–4 yr synchrony of defoliation					
	mean 2–4 yr power of neighbours	>−0.001	0.222	−0.002	0.998
	2–4 yr synchrony of PC1	−3.913	1.756	−2.229	0.026*
	2–4 yr synchrony of PC2	3.460	1.902	1.819	0.069
7–11 yr synchrony of defoliation					
	mean 7–11 yr power of neighbours	1.768	0.337	5.241	<0.001*
	7–11 yr synchrony of PC1	0.080	0.549	0.145	0.885
	7–11 yr synchrony of PC2	1.061	0.311	3.415	0.001*

Table 2. Results of generalized-least-squares regressions testing whether the timescale-specific local phase synchrony of gypsy moth defoliation between a focal location and neighbouring locations increases with the periodicity of defoliation in the neighbouring locations, while accounting for the effects of the local phase synchrony of weather (scores of two principal components) in neighbouring locations ($n = 1327$). (Significant p-values are highlighted with an asterisk (*).)

dependent variables	independent variables	coef.	s.e.	t	p-value
2–4 yr phase synchrony of defoliation					
	mean 2–4 yr power of neighbours	−0.056	0.056	−1.000	0.317
	2–4 yr phase synchrony of PC1	−0.444	0.296	−1.496	0.135
	2–4 yr phase synchrony of PC2	−0.102	0.620	−0.165	0.869
7–11 yr phase synchrony of defoliation					
	mean 7–11 yr power of neighbours	0.079	0.050	4.468	<0.001*
	7–11 yr phase synchrony of PC1	−0.002	0.037	−0.065	0.948
	7–11 yr phase synchrony of PC2	0.028	0.034	0.814	0.416

The significant positive effects of both population periodicity and weather spatial synchrony on population spatial synchrony at the 7–11 year timescales, and the positive effect of population periodicity on population phase synchrony at the same timescales, indicates that periodicity enhanced synchrony above and beyond the effect of environmental synchrony alone. Dispersal is the most commonly invoked mechanism of phase locking of population dynamics [6–8,11,53]. However, the spatial scale of our data relative to gypsy moth dispersal suggests that dispersal rates among neighbouring grid cells are insufficient to drive the phase-locking observed here. Adult females are flightless and larvae typically disperse only tens of metres [31]. Longer-range movements via human activities or entrainment in storms are possible [54–56], but are sporadic and rare. It is possible that movement of gypsy moth pathogens [57] or parasitoids could contribute to synchronization across this scale.

Consistent with previous research [22,44,58], our findings suggest the drivers of synchrony at one timescale can be different from the drivers of synchrony at other timescales. In our study system, the apparent effect of 7–11 year, but not 2–4 year, periodicity on the synchrony of gypsy moth outbreaks (table 1) may be explained by the fact that periodicity in defoliation was more prevalent at the 7–11 timescales than at the 2–4 year timescales (figure 1), given the theoretical prediction that local population cycling promotes population spatial synchrony [8,11,12]. Previous studies of gypsy moth temporal population dynamics have found considerable geographical variation in the strength of periodicity associated with heterogeneity in forest type [59], the density of preferred host trees [23] and elevation [60]. In the present study, we found that statistically significant periodicity in defoliation was detected at a sizeable proportion (greater than one-quarter) of locations (8×8 km grid cells) at the timescale of approximately 7.8 years (figure 1) and that the extent of geographical variation in the strength of periodicity was sufficient to reveal highly significant ($p < 0.001$) relationships between the strength of 7–11 year periodicity in defoliation and the synchrony and phase synchrony of defoliation (tables 1 and 2).

The stronger 7–11 year periodicity compared to 2–4 year periodicity could also explain why gypsy moth outbreaks displayed considerably stronger cross-wavelet synchrony at longer (0.88, 0.72–0.94; ; median, 1st quartile–3rd quartile) than shorter (0.48, 0.29–0.65) timescale ranges, but this

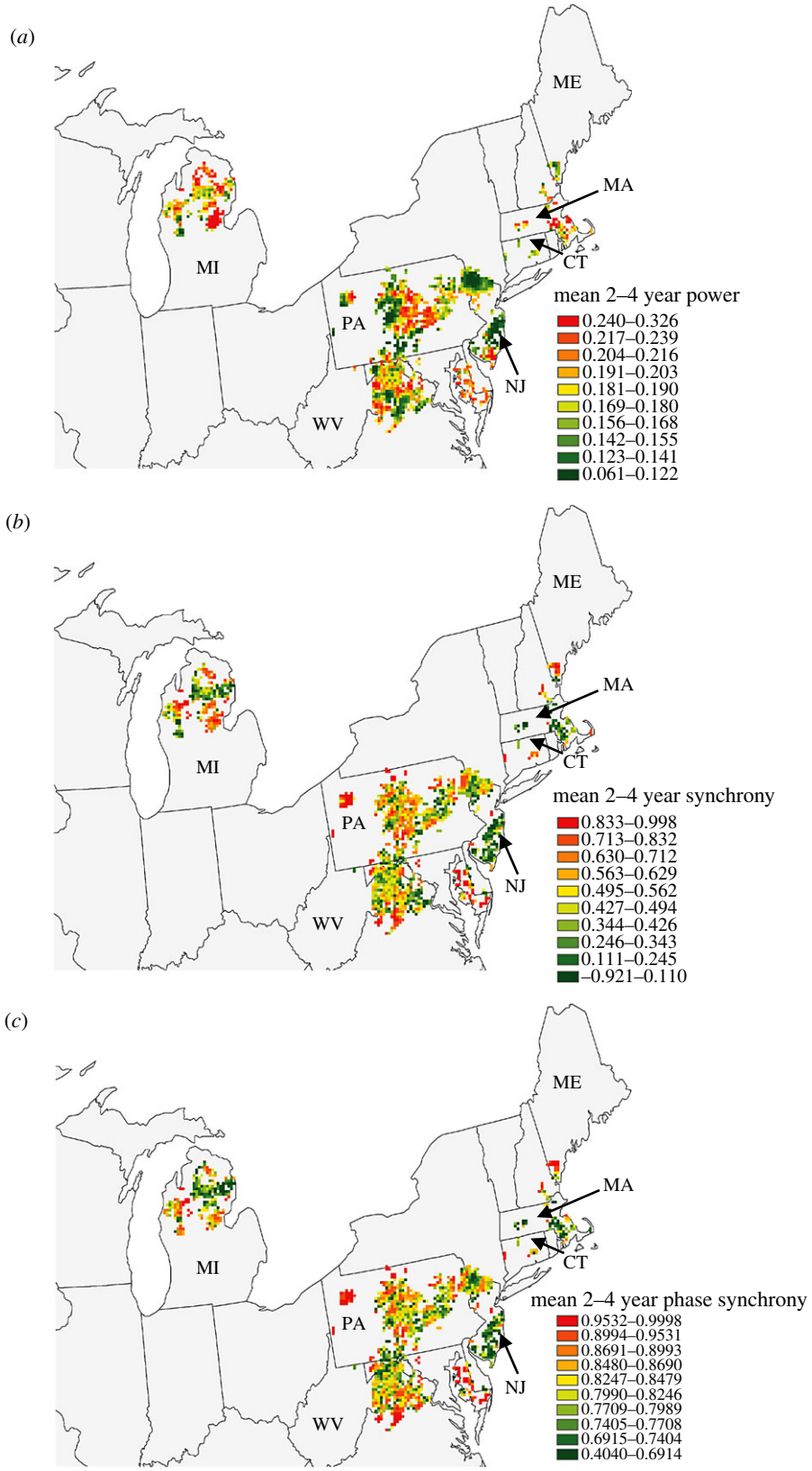

Figure 2. Spatial variation in the (*a*) periodicity (wavelet power), (*b*) synchrony and (*c*) phase synchrony of gypsy moth defoliation at the 2–4 year timescales. The value (colour category) displayed for each location (focal cell) is the mean value of the respective variable (power and synchrony) across the local neighbourhood of 1–8 cells adjacent to the focal cell. The cut off points dividing the colour categories shown in the legends were determined with quantile classification (i.e. all colour categories contain equal numbers of data values). State abbreviations: CT, Connecticut; ME, Maine, MA, Massachusetts; MI, MIchigan; NJ, New Jersey; PA, Pennsylvania; WV, West Virginia. (Online version in colour.)

difference in the strength of synchrony across timescales could also be a result of how well the dominant timescales of fluctuations in gypsy moth defoliation match those of the exogenous abiotic drivers, temperature and precipitation (largely represented by PC1 and PC2, respectively). There was little detuning (frequency mismatch) between the dominant timescales of fluctuations in defoliation (approx. 7–11 years) and that of precipitation (approx. 7–9 years, figure 1). In comparison, the detuning between the dominant timescales of gypsy moth outbreaks (approx. 7–11 years) and

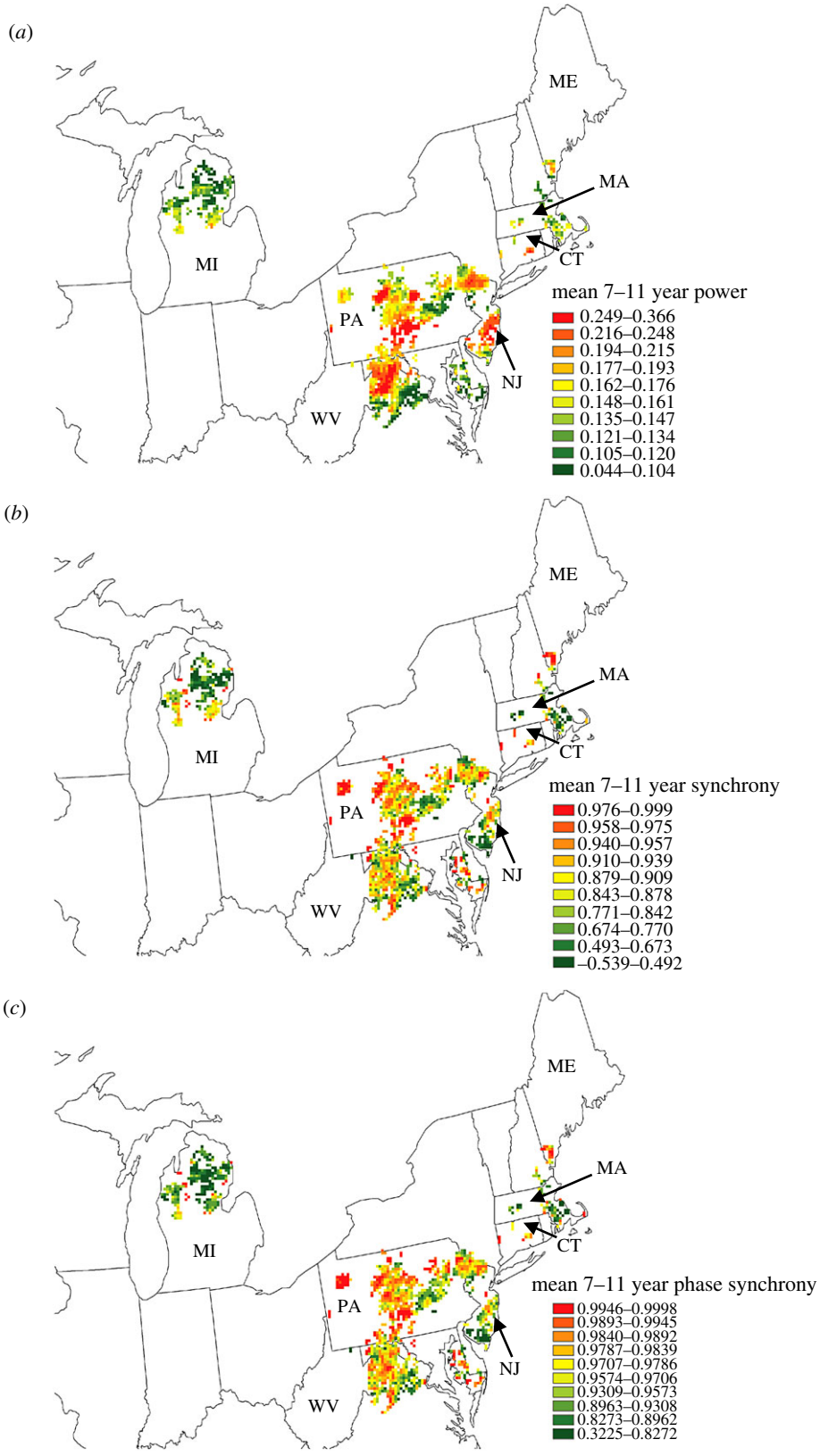

Figure 3. Spatial variation in the (*a*) periodicity (wavelet power), (*b*) synchrony and (*c*) phase synchrony of gypsy moth defoliation at the 7–11 year timescales. The value (colour category) displayed for each location (focal cell) is the mean value of the respective variable (power and synchrony) across the local neighbourhood of 1–8 cells adjacent to the focal cell. The cut off points dividing the colour categories shown in the legends were determined with quantile classification (i.e. all colour categories contain equal numbers of data values). For state abbreviations, see figure caption 2. (Online version in colour.)

temperature fluctuations (approx. 3.9 years) is considerably larger. The concept of detuning is clearly applicable to the study of how periodic macro-scale environmental forces (e.g. weather and the influences of teleconnection patterns such as the El Niño-Southern Oscillation) influence the synchrony of population dynamics, but further study in both experimental model systems and field populations is needed to evaluate its importance.

Partially synchronized fluctuations in precipitation at the 7–11 year timescales appears to be the main abiotic driver of population synchrony in our study, but we also found that the 2–4 year synchrony of gypsy moth outbreaks was

inversely related to the 2–4 year synchrony of temperature. No previous studies have reported effects of temperature on the synchrony of gypsy moth outbreaks [20,21,42], we found no evidence that temperature affects the phase synchrony of defoliation (table 2), and we are unaware of any processes whereby synchrony in the fluctuations of an abiotic factor at a given timescale would reduce the synchrony of population fluctuations at the same timescale. For these reasons, we suspect the negative relationship between the synchronies of temperature and defoliation that we detected was spurious.

The approaches and concepts used here represent new avenues to understand the role of cyclic population dynamics, and other timescale-specific drivers, in population synchrony. As the distances over which nonlinear phase locking can operate are unclear—theory suggests these distances are infinite but local heterogeneity in population dynamics and increasing asynchrony in environmental perturbations with increasing distance suggest the phase locking may occur only over short distances [11,53]—future work should explore how the drivers of timescale-specific synchrony vary across different spatial scales. More broadly, such an approach would allow exploration of the changes in the relative importance of different drivers of synchrony (e.g. environmental forcing and dispersal) across local to regional spatial scales.

Data accessibility. All data are available from the Dryad Data Repository: https://doi.org/10.5061/dryad.j6h230v [61]. The R code for measuring local synchrony and phase synchrony are available from GitHub at: https://github.com/jonathan-walter/wavelet-nclisa [62].

Authors' contributions. K.J.H. and J.A.W. conceived the study. K.J.H., J.A.W. and A.M.L. contributed to the plans for data analysis. A.M.L. coordinated the compilation of the defoliation and weather data. J.A.W. wrote the software code for the statistical analysis of timescale-specific synchrony and phase synchrony. K.J.H. carried out the statistical analyses and wrote the first draft of the manuscript, except the portions that J.A.W. wrote describing the newly developed statistical analyses. All authors contributed substantially to revisions.

Competing interests. We declare we have no competing interests.

Funding. J.A.W. was supported by a NatureNet Science Fellowship from The Nature Conservancy and the University of Virginia, and USDA grant 2016-67012-24694. A.M.L. acknowledges support from EVA4.0, no. CZ.02.1.01/0.0/0.0/16_019/0000803 financed by OP RDE.

Acknowledgements. We thank Ottar Bjørnstad for sharing useful insights as this project was being envisioned and Eugene Luzader for data compilation and assistance with figures.

References

1. Liebhold A, Koenig WD, Bjørnstad ON. 2004 Spatial synchrony in population dynamics. *Annu. Rev. Ecol. Evol. Syst.* **35**, 467–490. (doi:10.1146/annurev.ecolsys.34.011802.132516)
2. Earn DJD, Levin SA, Rohani P. 2000 Coherence and conservation. *Science* **290**, 1360–1364. (doi:10.1126/science.290.5495.1360)
3. de Valpine P, Scranton K, Ohmart CP. 2010 Synchrony of population dynamics of two vineyard arthropods occurs at multiple spatial and temporal scales. *Ecol. Appl.* **20**, 1926–1935. (doi:10.1890/09-0468.1)
4. Ranta E, Kaitala V, Lundberg P. 1997 The spatial dimension in population fluctuations. *Science* **278**, 1621–1623. (doi:10.1126/science.278.5343.1621)
5. Lindström J, Ranta E, Lindén H. 1996 Large-scale synchrony in the dynamics of capercaillie, black grouse and hazel grouse populations in Finland. *Oikos* **76**, 221–227. (doi:10.2307/3546193)
6. Vasseur DA, Fox JW. 2009 Phase-locking and environmental fluctuations generate synchrony in a predator-prey community. *Nature* **460**, 1007–1U90. (doi:10.1038/nature08208)
7. Bjørnstad ON. 2000 Cycles and synchrony: two historical 'experiments' and one experience. *J. Anim. Ecol.* **69**, 869–873. (doi:10.1046/j.1365-2656.2000.00444.x)
8. Ranta E, Kaitala V, Lundberg P. 1998 Population variability in space and time: the dynamics of synchronous population fluctuations. *Oikos* **83**, 376–382. (doi:10.2307/3546852)
9. Blasius B, Huppert A, Stone L. 1999 Complex dynamics and phase synchronization in spatially extended ecological systems. *Nature* **399**, 354–359. (doi:10.1038/20676)
10. Pikovsky A, Rosenblum M, Kurths J. 2001 *Synchronization: a universal concept in nonlinear sciences*. Cambridge, UK: Cambridge University Press.
11. Jansen VAA. 1999 Phase locking: another cause of synchronicity in predator–prey systems. *Trends Ecol. Evol.* **14**, 278–279. (doi:10.1016/S0169-5347(99)01654-7)
12. Bjørnstad ON, Ims RA, Lambin X. 1999 Spatial population dynamics: analyzing patterns and processes of population synchrony. *Trends Ecol. Evol.* **14**, 427–432. (doi:10.1016/S0169-5347(99)01677-8)
13. Cazelles B, Boudjema G. 2001 The Moran effect and phase synchronization in complex spatial community dynamics. *Am. Nat.* **157**, 670–676. (doi:10.1086/320624)
14. Mosekilde E, Maistrenko Y, Postnov D. 2002 *Chaotic synchronization: applications to living systems*. River Edge, NJ: World Scientific Publishing, Co. Pte. Ltd.
15. Steen H, Yoccoz NG, Ims RA. 1990 Predators and small rodent cycles: an analysis of a 79-year time series of small rodent population fluctuations. *Oikos* **59**, 115–120. (doi:10.2307/3545130)
16. Rohani P, Earn DJD, Grenfell BT. 1999 Opposite patterns of synchrony in sympatric disease metapopulations. *Science* **286**, 968–971. (doi:10.1126/science.286.5441.968)
17. Henden J-A, Ims RA, Yoccoz NG. 2009 Nonstationary spatio-temporal small rodent dynamics: evidence from long-term Norwegian fox bounty data. *J. Anim. Ecol.* **78**, 636–645. (doi:10.1111/j.1365-2656.2008.01510.x)
18. Campbell RW. 1974 *The gypsy moth and its natural enemies. Agriculture Information Bulletin No. 381*. Washington, DC: US Department of Agriculture.
19. Dwyer G, Dushoff J, Yee SH. 2004 The combined effects of pathogens and predators on insect outbreaks. *Nature* **430**, 341–345. (doi:10.1038/nature02569)
20. Haynes KJ, Bjørnstad ON, Allstadt AJ, Liebhold AM. 2013 Geographical variation in the spatial synchrony of a forest-defoliating insect: isolation of environmental and spatial drivers. *Proc. R. Soc. B* **280**, 20122373. (doi:10.1098/rspb.2012.2373)
21. Haynes KJ, Liebhold AM, Bjørnstad ON, Allstadt AJ, Morin RS. 2018 Geographic variation in forest composition and precipitation predict the synchrony of forest insect outbreaks. *Oikos* **127**, 634–642. (doi:10.1111/oik.04388)
22. Defriez EJ, Reuman DC. 2017 A global geography of synchrony for terrestrial vegetation. *Glob. Ecol. Biogeogr.* **26**, 878–888. (doi:10.1111/geb.12595)
23. Haynes KJ, Liebhold AM, Johnson DM. 2009 Spatial analysis of harmonic oscillation of gypsy moth outbreak intensity. *Oecologia* **159**, 249–256. (doi:10.1007/s00442-008-1207-7)
24. Liebhold A, Elkinton J, Williams D, Muzika R. 2000 What causes outbreaks of the gypsy moth in North America? *Popul. Ecol.* **42**, 257–266. (doi:10.1007/PL00012004)
25. Peltonen M, Liebhold AM, Bjørnstad ON, Williams DW. 2002 Spatial synchrony in forest insect outbreaks: roles of regional stochasticity and dispersal. *Ecology* **83**, 3120–3129. (doi:10.1890/0012-9658(2002)083[3120:SSIFIO]2.0.CO;2)
26. Haynes KJ, Liebhold AM, Fearer TM, Wang G, Norman GW, Johnson DM. 2009 Spatial synchrony propagates through a forest food web via consumer-resource interactions. *Ecology* **90**, 2974–2983. (doi:10.1890/08-1709.1)

27. Elkinton J, Liebhold A. 1990 Population dynamics of gypsy moth in North-America. *Annu. Rev. Entomol.* **35**, 571–596. (doi:10.1146/annurev.ento.35.1.571)
28. Hajek AE, Tobin PC, Haynes KJ. 2015 Replacement of a dominant viral pathogen by a fungal pathogen does not alter the collapse of a regional forest insect outbreak. *Oecologia* **177**, 785–797. (doi:10.1007/s00442-014-3164-7)
29. Hajek AE. 1999 Pathology and epizootiology of the Lepidoptera-specific mycopathogen *Entomophaga maimaiga*. *Microbiol. Mol. Biol. Rev.* **63**, 14–835.
30. Liebhold AM, Plymale R, Elkinton JS, Hajek AE. 2013 Emergent fungal entomopathogen does not alter density dependence in a viral competitor. *Ecology* **94**, 1217–1222. (doi:10.1890/12-1329.1)
31. Mason CJ, McManus ML. 1981 Larval dispersal of the gypsy moth. In *The gypsy moth: research toward integrated pest management*, pp. 161–202. Washington, DC: US Department of Agriculture.
32. Williams DW, Fuester RW, Metterhouse WW, Balaam RJ, Bullock RH, Chianesei RJ. 1991 Oak defoliation and population density relationships for the gypsy moth (Lepidoptera: Lymantriidae. *J. Econ. Entomol.* **84**, 1508–1514. (doi:10.1093/jee/84.5.1508)
33. Liebhold AM, Simons EE, Sior A, Unger JD. 1993 Forecasting defoliation caused by the gypsy moth from field measurements. *Environ. Entomol.* **22**, 26–32. (doi:10.1093/ee/22.1.26)
34. Liebhold AM, Gottschalk KW, Mason DA, Bush RR. 1997 Forest susceptibility of the gypsy moth. *J. For.* **95**, 20–24.
35. R Core Team. 2018 *R: a language and environment for statistical computing*. Vienna, Austria: R Foundation for Statistical Computing.
36. Torrence C, Compo GP. 1998 A practical guide to wavelet analysis. *Bull. Am. Meteorol. Soc.* **79**, 61–78. (doi:10.1175/1520-0477(1998)079<0061:APGTWA>2.0.CO;2)
37. Liu Y, San Liang X, Weisberg RH. 2007 Rectification of the bias in the wavelet power spectrum. *J. Atmospheric Ocean. Technol.* **24**, 2093–2102. (doi:10.1175/2007JTECHO511.1)
38. Sardeshmukh PD, Compo GP, Penland C. 2000 Changes of probability associated with El Niño. *J. Clim.* **13**, 4268–4286. (doi:10.1175/1520-0442(2000)013<4268:COPAWE>2.0.CO;2)
39. Cazelles B, Chavez M, Constantin de Magny G, Guégan J-F, Hales S. 2007 Time-dependent spectral analysis of epidemiological time-series with wavelets. *J. R. Soc. Interface* **4**, 625–636. (doi:10.1098/rsif.2007.0212)
40. Cazelles B, Cazelles K, Chavez M. 2014 Wavelet analysis in ecology and epidemiology: impact of statistical tests. *J. R. Soc. Interface* **11**, 20130585. (doi:10.1098/rsif.2013.0585)
41. Gouveia AR, Bjørnstad ON, Tkadlec E. 2016 Dissecting geographic variation in population synchrony using the common vole in central Europe as a test bed. *Ecol. Evol.* **6**, 212–218. (doi:10.1002/ece3.1863)
42. Walter JA, Sheppard LW, Anderson TL, Kastens JH, Bjørnstad ON, Liebhold AM, Reuman DC. 2017 The geography of spatial synchrony. *Ecol. Lett.* **20**, 801–814. (doi:10.1111/ele.12782)
43. Jammalamadaka SR, SenGupta A. 2001 *Topics in circular statistics*. Singapore: World Scientific Publishing, Co. Pte. Ltd.
44. Sheppard LW, Bell JR, Harrington R, Reuman DC. 2016 Changes in large-scale climate alter spatial synchrony of aphid pests. *Nat. Clim. Change* **6**, 610–613. (doi:10.1038/nclimate2881)
45. Reuman DC, Anderson TL, Walter JA, Zhao L, Sheppard LW. 2018 wsyn: Wavelet approaches to studies of synchrony in ecology and other fields. See https://github.com/reumandc/wsyn
46. Agostinelli C, Lund U. 2017 R package 'circular': circular statistics (version 0.4-93). See https://r-forge.r-project.org/projects/circular/.
47. Bjørnstad ON. 2018 ncf: spatial covariance functions. See https://CRAN.R-project.org/package=ncf.
48. Pinheiro J, Bates D, DeBroy S, Sarkar D, R Core Team. 2016 nlme: linear and nonlinear mixed effects models. See http://CRAN.R-project.org/package=nlme.
49. Grenfell BT, Wilson K, Finkenstädt BF, Coulson TN, Murray S, Albon SD, Pemberton JM, Clutton-Brock TH, Crawley MJ. 1998 Noise and determinism in synchronized sheep dynamics. *Nature* **394**, 674–677. (doi:10.1038/29291)
50. Ranta E, Veijo K, Lindströom J. 1999 Spatially autocorrelated disturbances and patterns in population synchrony. *Proc. R. Soc. Lond. B* **266**, 1851–1856. (doi:10.1098/rspb.1999.0856)
51. D'Amico V, Elkinton J. 1995 Rainfall effects on transmission of gypsy moth (Lepidoptera, Lymantriidae) nuclear polyhedrosis virus. *Environ. Entomol.* **24**, 1144–1149. (doi:10.1093/ee/24.5.1144)
52. Reilly JR, Hajek AE, Liebhold AM, Plymale R. 2014 Impact of *Entomophaga maimaiga* (Entomophthorales: Entomophthoraceae) on outbreak gypsy moth populations (Lepidoptera: Erebidae): the role of weather. *Environ. Entomol.* **43**, 632–641. (doi:10.1603/EN13194)
53. Fox JW, Vasseur DA, Hausch S, Roberts J. 2011 Phase locking, the Moran effect and distance decay of synchrony: experimental tests in a model system. *Ecol. Lett.* **14**, 163–168. (doi:10.1111/j.1461-0248.2010.01567.x)
54. Tobin PC, Blackburn LM. 2008 Long-distance dispersal of the gypsy moth (Lepidoptera: Lymantriidae) facilitated its initial invasion of Wisconsin. *Environ. Entomol.* **37**, 87–93. (doi:10.1603/0046-225X(2008)37[87:LDOTGM]2.0.CO;2)
55. Bigsby KM, Tobin PC, Sills EO. 2011 Anthropogenic drivers of gypsy moth spread. *Biol. Invasions* **13**, 2077–2090. (doi:10.1007/s10530-011-0027-6)
56. Frank KL, Tobin PC, Thistle HW, Kalkstein LS. 2013 Interpretation of gypsy moth frontal advance using meteorology in a conditional algorithm. *Int. J. Biometeorol.* **57**, 459–473. (doi:10.1007/s00484-012-0572-4)
57. Bittner TD, Hajek AE, Liebhold AM, Thistle H. 2017 Modification of a pollen trap design to capture airborne conidia of *Entomophaga maimaiga* and detection of conidia by quantitative PCR. *Appl Env. Microbiol* **83**, e00724-17. (doi:10.1128/AEM.00724-17)
58. Keitt TH. 2008 Coherent ecological dynamics induced by large-scale disturbance. *Nature* **454**, 331–334. (doi:10.1038/nature06935)
59. Johnson D, Liebhold A, Bjørnstad O. 2006 Geographical variation in the periodicity of gypsy moth outbreaks. *Ecography* **29**, 367–374. (doi:10.1111/j.2006.0906-7590.04448.x)
60. Haynes KJ, Liebhold AM, Johnson DM. 2012 Elevational gradient in the cyclicity of a forest-defoliating insect. *Popul. Ecol.* **54**, 239–250. (doi:10.1007/s10144-012-0305-x)
61. Haynes KJ, Walter JA, Liebhold AM. 2019 Data from: Population spatial synchrony enhanced by periodicity and low detuning with environmental forcing. Dryad Digital Repository. (https://doi.org/10.5061/dryad.j6h230v)
62. Walter JA. 2019 Wavelet-nclisa. GitHub. See https://github.com/jonathan-walter/wavelet-nclisa.